Supplementary Information

Bio-augmented Additive Manufacturing of Engineered Living Materials with Mechanical Enhancement and Resistance to Degradation

Gokce Altin-Yavuzarslan[1], Sierra M. Brooks[2], Shuo-FuYuan[3], James O. Park[3], Hal S. Alper[2,3*], Alshakim Nelson[1,5*]

[1]Molecular Engineering and Sciences Institute, University of Washington, Seattle, Washington 98195, United States
[2]McKetta Department of Chemical Engineering, The University of Texas at Austin, Austin, TX, USA
[3]Institute for Cellular and Molecular Biology, The University of Texas at Austin, Austin, TX, USA
[4]Department of Surgery, University of Washington, Seattle, Washington 98195, United States.
[5]Department of Chemistry, University of Washington, Box 351700, Seattle, WA, USA

*Corresponding Authors:
Prof. Hal S. Alper
Institute for Cellular and Molecular Biology, The University of Texas at Austin, Austin, TX, USA
E-mail: halper@che.utexas.edu
Prof. Alshakim Nelson
Department of Chemistry, University of Washington, Box 351700, Seattle, WA, USA
E-mail: alshakim@uw.edu

This document includes:

Supporting experimental details, discussion, and references

1. Supporting experimental details and discussion

The effect of PEGDA concentration and presence of microbial culture on printability of BSA-PEGDA conjugates were determined by characterization of rheological properties of resin formulations (Supplementary Table 3). In all formulations, resin viscosities were found ≤ 1 Pa. s. After the addition of microbial culture media, resins were stirred for 30 min at 200 rpm to maintain homogenous distribution of microorganism in the resin. It has been observed that when the 30 wt% BSA, 10 wt% PEGDA formulation was stirred for 30 min at 200 rpm the viscosity was changed 1.0 Pa. s (Entry 3, Supplementary Table 3) to 0.35 Pa. s (Entry 4, Supplementary Table 3). Therefore, it may be said that the viscosity reduction of Entry 5, Entry 6, Entry 7, and Entry 8 was mainly caused by stirring step rather than the addition of microorganism or culture media to the resin formulation. According to the findings, Entry 1 and Entry 2 required longer time, 47.5 s and 20 s, respectively, to reach the crossover point compared to other formulations (Supplementary Table 3). This longer time is not desirable to obtain 3D printed constructs in SLA 3D printers (Supplementary Fig. 1a). When PEGDA concentration was increased from 3 wt% to 10 wt%, the resin reached the crossover point at least 10 times faster (Entry 3, Supplementary Table 3). Presence of more PEGDA units in 30 wt% BSA, 10 wt% PEGDA formulation led to the reaction of the acrylate groups with each other more easily. Therefore, this formulation provided faster photocuring rate and shorter time to achieve crossover point (Entry 3, Supplementary Table 3). 3D printed objects were successfully obtained with formulation 30 wt% BSA, 10 wt% PEGDA (Supplementary Fig. 1b). In ELM formulations (Entry 6, and Entry 8, Supplementary Table 3,) both stirring step (30 min at 200 rpm) and presence of microbial culture could affect the time to reach crossover point and rate of photocuring (Entry 6 and Entry 8, Supplementary Table 3). On the other hand, these changes did not affect the SLA.

To understand the effect of bioactive compounds produced from metabolically engineered cells on the BSA-PEGDA network, possible interactions between bioactive components and BSA were evaluated with UV-absorbance measurements. Supplementary Fig. 5 represents the interaction of L-DOPA to BSA. The samples prepared as follows, BSA (0.5 mg/ml in DI water), L-DOPA (0.5 mg/ml in DI water), BSA+L-DOPA (0.5 mg/ml for each component in DI water). Supplementary Fig. 6 shows the interaction of naringenin (NGN) to BSA. The samples prepared as follows, BSA (0.5 mg/ml in DI water). 100 mg/ml NGN stock solution was prepared in ethanol and diluted in water to 0.5 mg/ml. BSA+NGN sample contained 0.5 mg/ml for each component and prepared in DI water.

We observed that *in-situ* betaxanthins (BXN) production prevented microbial degradation, as both BSA-PEGDA and ELM-SC-BXN showed a similar trend in terms of mass change over 45 d. Two possible mechanisms of actions can be responsible to this resistance: binding of BXN to degradation enzymes such as proteinase or binding of BXN to BSA.[1-3] We selected ProK as a model enzyme to examine the binding of BXN to microbial enzymes. The binding of BXN to BSA and ProK was confirmed by UV-vis absorbance and CD-spectroscopy. The absorbance of both proteins, as well as BXN, was changed after they interact with each other Supplementary Fig. 7 and Supplementary Fig. 8. In addition, the binding of BXN to BSA resulted in the loss of the α-helical structure of BSA. The characteristic spectrum of α-helix motif in the negative region at between 222 to 208 nm disappeared in the presence of BXN (Fig. 5b). Similarly, conformational changes were observed in ProK after the binding of BXN to this protein (Supplementary Fig. 0). The weak negative peak between 230 to 220 nm belongs to β-turns[2] and the β-sheet motif in ProK[2] was identified (Supplementary Fig 12). In the presence of BXN, the characteristic CD spectra of ProK were completely changed. BXN alter the structural motifs, both β-sheets, and β-turns, of ProK.

Literature Cited

[1] S. Paudyal, G. Sigdel, S. K. Shah, S. K. Sharma, J. D. Grubb, M. Micic, L. Caseli, R. M. Leblanc, *J Colloid Interface Sci* **2022,** *616,* 701-708.

[2] J. Liu, H. Yong, X. Yao, H. Hu, D. Yun, L. Xiao, *RSC Adv* **2019**, 9, 35825-35840.

[3] M. I. Khan, P. Giridhar, *Phytochemistry* **2015,** *117,* 267-295.

[4] S. Zhou, S. F. Yuan, P. H. Nair, H. S. Alper, Y. Deng, J. Zhou, *Metab Eng* **2021,** *67,* 41-52.

[5] T. G. Johnston, S. F. Yuan, J. M. Wagner, X. Yi, A. Saha, P. Smith, A. Nelson, H. S. Alper, Nat Commun **2020**, *11,* 1-11.

Supplementary Table 1. Name of 3D printed ELM samples, the microorganisms that each sample contains, and the bioactive compound that is produced from each microorganism.

Sample	Microorganisms	Bioactive compound
ELM-SC-WT	Wild type *S. cerevisiae*	-
ELM-SC-WT	Wild type *E. coli*	-
ELM-SC-BXN	*S. cerevisiae* BY4741	Betaxanthin
ELM-EC-LDOPA	*E. coli*e BL0430D	L-DOPA
ELM-EC-NGN	*E. coli* BL21(DE3)	Naringenin

Supplementary Table 2. Description of strains and plasmids

Strain/plasmid	Description	Source
E. coli strains		
BL21(DE3)	E. coli str. B F– ompT gal dcm lon hsdSB($r_B^-m_B^-$) λ (DE3 [lacI lacUV5- T7p07 ind1 sam7 nin5]) [$malB^+$]$_{K-12}$(λ^S)	New England Biolabs
E. coli BL21(DE3) Mut-17	[BL21(DE3)]: pETM-PUTRtrxA-TAL-PUTRtalB-4CL, pCDM-PssrA-UTRrpsT-CHS-PUTRglpD-CHI, pACM-PfdeR-mut-FdeR-PfdeA-mut-acpH-asacpT-asacpS, and pRSM-PcspA-mut-PadR-acs-ACC (KanR, AmpR, SpcR, CmR)	Reference [4]
eBL0430D	[E. coli BL21(DE3)] ΔtyrR , pET28-pYIBN-aroG(fbr)-B30rbs-tyrA(fbr)-tRRNC; KanR , pCDF-pLPP-B30rbs-hpaB-hpaC-T7t; KanR; SpcR	Reference [5]
S. cerevisiae strains		
BY4741	MATα SUC2 gal2 mal2 mel flo1 flo8-1 hap1 ho bio1 bio6 his3Δ1 leu2Δ0 met15Δ0 ura3Δ0	American Type Culture Collection (ATCC)
BY01	*S. Cerevisiae* BY4741: ura3:pCCW12-MjDOD(T261N; ACC to AAC)-pTDH3-CYP76AD5 -tPRM9 (URA3integration with Leu2 marker)	This Study
Plasmids		
pET28-pYIBN-aroG(fbr)-B30rbs-tyrA(fbr)-tRRNC. KanR	For L-DOPA production	Reference [5]
pCDF-pLPP-B30rbshpaB-hpaC-T7t. SpcR	For L-DOPA production	Reference [5]
pETM-PUTRtrxA-TAL-PUTRtalB-4CL	For Naringenin production	Reference [4]
pCDM-PssrA-UTRrpsT-CHS-PUTRglpD-CHI	For Naringenin production	Reference [4]
pACM-PfdeR-mut-FdeR-PfdeA-mut-acpH-asacpT-asacpS	For Naringenin production	Reference [4]
pRSM-PcspA-mut-PadR-acs-ACC	For Naringenin production	Reference [4]

Supplementary Table 3. Primers and sequences

Primer	Sequence (5'-3')
P1	GTGGTTTCAGGGTCCATAAAGCgagctcCTGAACTGGCCGATAATTGC
P2	gatgcgtaaggagaaaataccgcatcaggTAGGTTGTCTGTGCCCATAC
P3	CCTGATGCGGTATTTTCTCCTTACG
P4	GAGCTCGCTTTATGGACCCTG
P5	GAAGGATAAGTTTTGACCATCAAAG
P6	GGTGAAGTTGTAGGTAGAGTAACC

Supplementary Table 4. Effect of PEGDA concentration and microbial culture media on rheological properties and SLA 3D printability of BSA-PEGDA conjugates.

Entry	BSA wt. %	PEGDA wt. %	Microbial Culture Media	Viscosity (Pa s)	G' rate change (Pa/s)	Crossover point (s)	Printability
1	30	3	-	0.17	0.003	47.5	No
2	30	5	-	0.40	70.45	20.0	No
3	30	10	-	1.00	2884.1	4.0	Yes
4*	30	10	-	0.35	-	-	Yes
5	30	10	LB	0.27	3535.07	10.0	Yes
6	30	10	*E. coli*	0.13	1238.82	13.5	Yes
7	30	10	YPD	0.35	1088.56	8.0	Yes
8	30	10	*S. cerevisiae*	0.30	1620.55	12.0	Yes

* Entry 4 was stirred for 30 min before measurement similar to Entry 5-8. These samples were stirred after the addition of microbial culture and/or culture media to provide the homogenous distribution of added compounds to resin formulation.

Supplementary Table 5. Degree of swelling of SLA 3D printed samples. (Samples were prepared in triplicate, (± s.d).

Sample	Degree of Swelling (q)
BSA-PEGDA in LB media	1.56 ± 0.05
ELM-EC-LDOPA	1.34 ± 0.01
ELM-EC-WT	1.56 ± 0.07
BSA-PEGDA+L-DOPA	1.33 ± 0.17
ELM-EC-NGN	2.70 ± 0.4
BSA-PEGDA+NGN	1.10 ± 0.01
BSA-PEGDA in YPD media	1.63 ± 0.03
ELM-SC-BXN	1.61 ± 0.07
ELM-SC-WT	1.89 ± 0.01

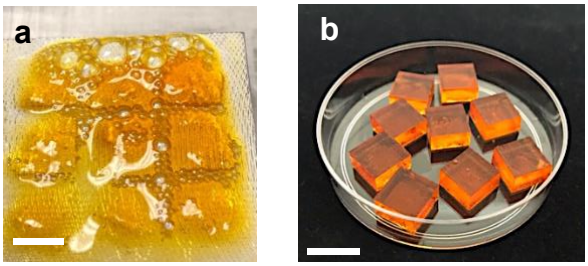

Supplementary Figure 1. Optical images of SLA 3D printed constructs. (a) Formulation of 30 wt% BSA with 5 wt% PEGDA (Entry 2, Table S2), unsuccessful printing, delamination was observed. (b) Formulation of 30 wt% BSA with 10 wt% PEGDA (Entry 3, Table S2), printing was successfully completed.

231
232

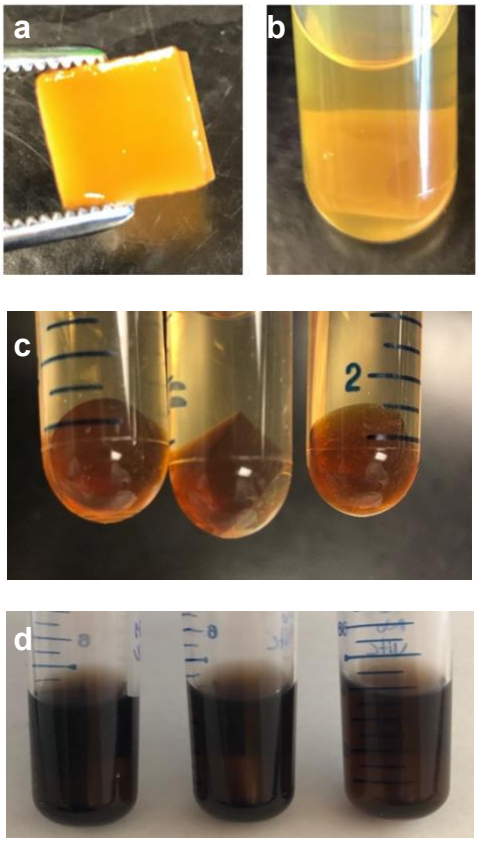

Supplementary Figure 2. Optical images of ELM samples after culturing. (a) ELM-SC-BXN cultured in YPD for 1 d, (b) ELM-SC-BXN in YPD, cultured for 1 d, (c) ELM-EC-LDOPA in vitamin C supplemented LB media cultured for 1 d, (d) ELM-EC-LDOPA in LB media cultured for 1 d.

253
254

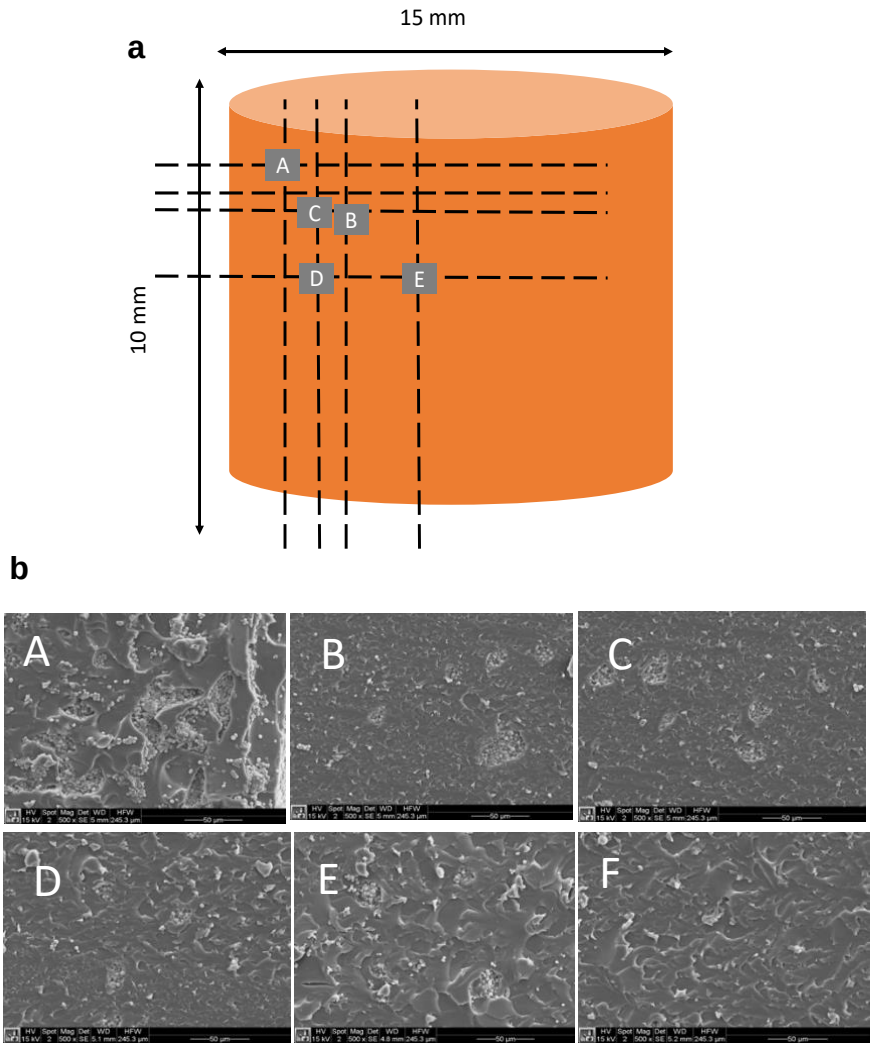

Supplementary Figure 3. Distribution of cells in SLA 3D printed ELM construct. (a), Schematic illustration of ELM-SC-BXN sample and location of each section that was imaged in the scanning electron microscope (SEM), (b) SEM images of *S. cerevisiae* in ELM-SC-BXN, images were taken at 500x magnification.

255
256

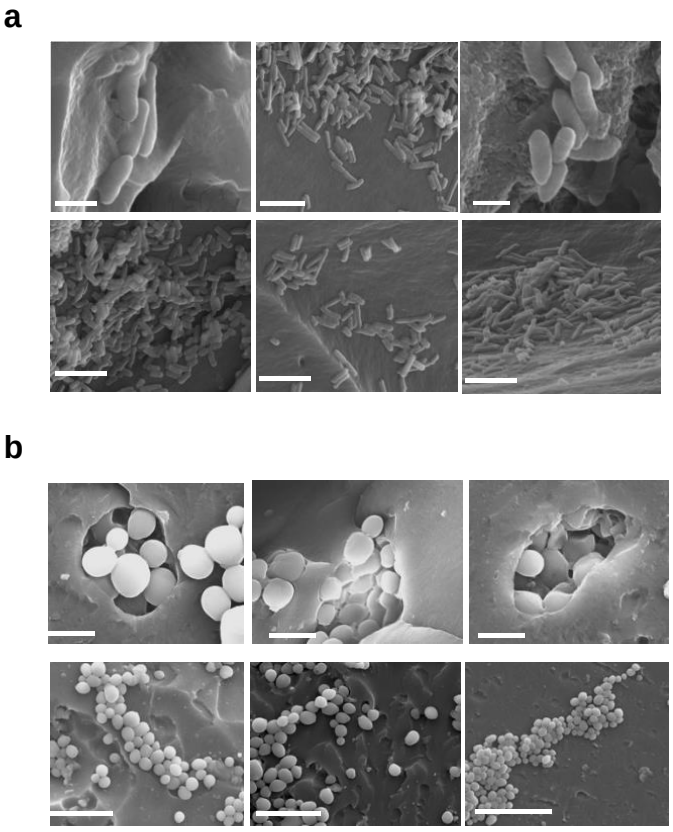

Supplementary Figure 4. Morphology of cells in 3D printed ELMs. (a) SEM images of *E. coli* in 3D printed ELM-EC-LDOPA constructs at different magnifications; 1000X magnification (scale bar 20 micron), 5000X (scale bar 5 micron), 20000X (scale bar 1 micron), (b) SEM images of *S. cerevisiae* in 3D printed ELM-SC-BXN constructs at different magnifications; 1500X magnification (scale bar 20 micron), 2500X (scale bar 10 micron), 7000X (scale bar 2 micron).

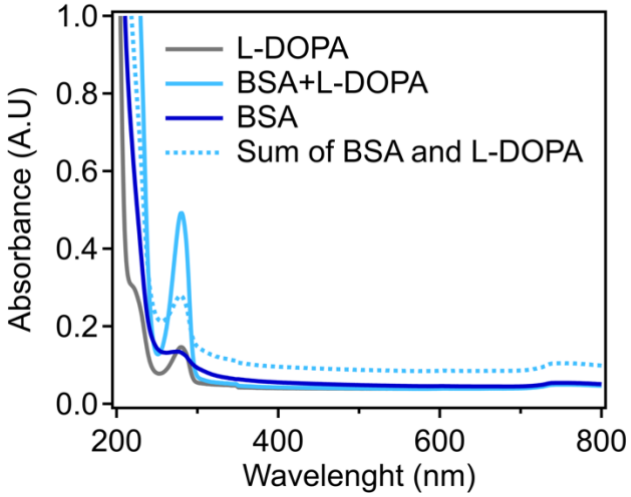

Supplementary Figure 5. Interaction of L-DOPA to BSA. UV-absorption spectra of BSA, L-DOPA, sum of individual spectra of BSA and L-DOPA, and spectra of BSA+L-DOPA mixture.

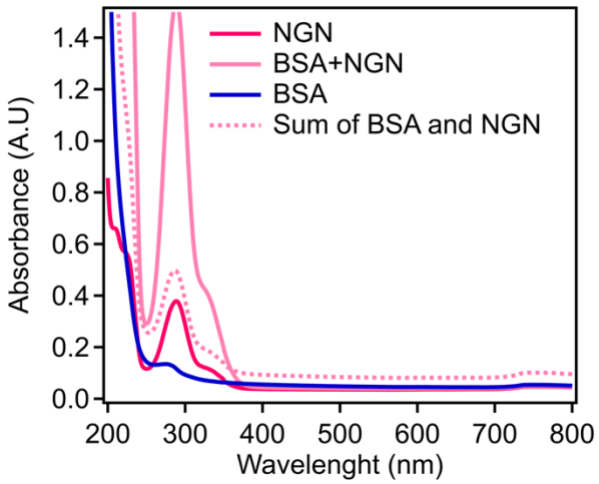

Supplementary Figure 6. Interaction of naringenin (NGN) to BSA. UV-absorption spectra of BSA, NGN, sum of individual spectra of BSA and NGN, and spectra of BSA+NGN mixture.

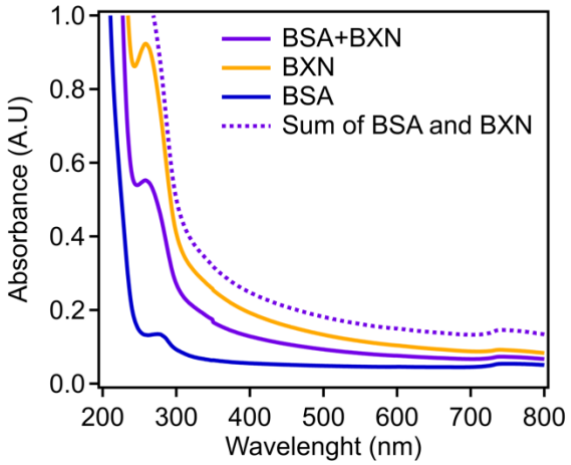

Supplementary Figure 7. Interaction of betaxanthins (BXN) to BSA. UV-absorption spectra of BSA, BXN, sum of individual spectra of BSA and BXN, and spectra of BSA+BXN mixture.

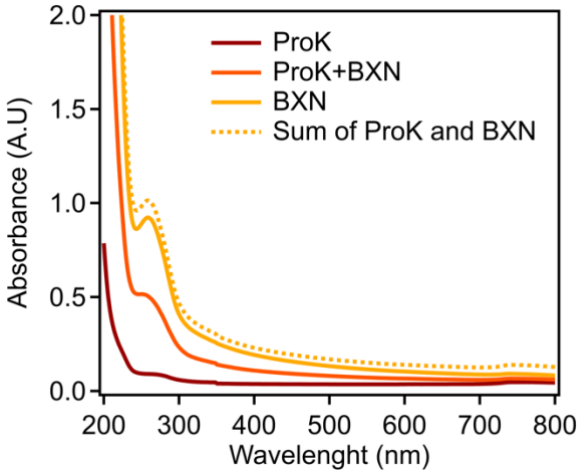

Supplementary Figure 8. Interaction of betaxanthins (BXN) to Proteinase K (ProK). UV-absorption spectra of ProK, BXN, sum of individual spectra of ProK and BXN, and spectra of ProK+BXN mixture.

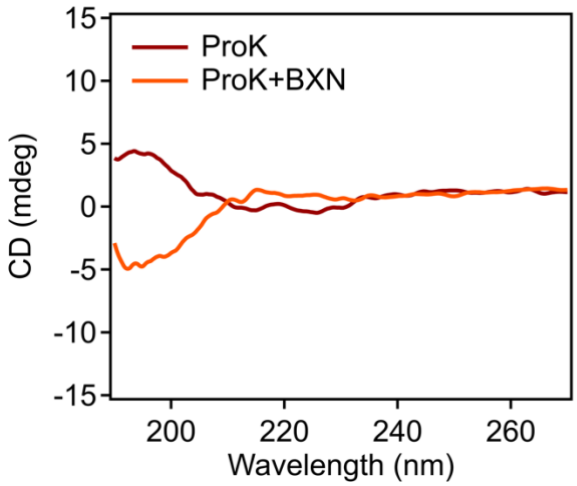

Supplementary Figure 9. Effect of betaxanthins (BXN) on the secondary structure of Proteinase K (ProK). CD spectra of ProK and CD spectra of ProK with the presence of BXN (ProK+BXN).

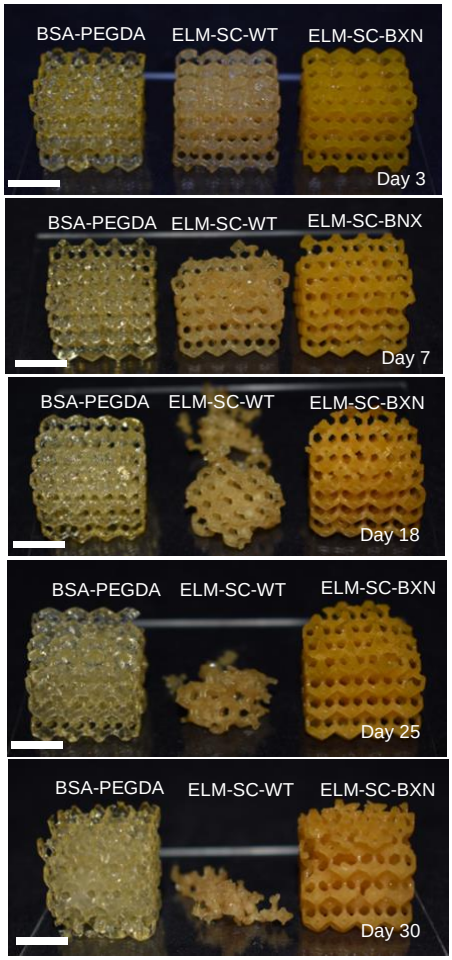

Supplementary Figure 10. Degradation of BSA-PEGDA, ELM-SC-WT and ELM-SC-BXN samples over 30 d.

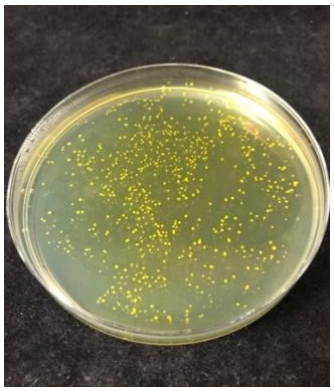

Supplementary Figure 11. The long-term viability of cells in ELM-SC-BXN (samples collected on day 40).